Selection of ionization paths of K_2 on superfluid helium droplets by wave packet interference

Marek Bastian Hild, Adrien Dufour[1], Georg Achazi[2], Alexander Patas, Paul Scheier[3], Albrecht Lindinger*

Institut für Experimentalphysik, Freie Universität Berlin, Arnimallee 14, 14195 Berlin, Germany

Abstract

We report on the control of wave packet dynamics for the ionization of K_2 attached to the surface of superfluid helium droplets. The superfluid helium matrix acts as a heat sink and reduces the coherence time of molecular processes by dissipation. We use tailor-shaped pulses in order to activate or inhibit different ionization paths by constructive or destructive wave packet interference. A drastic change of the wave packet dynamics is observed by shifting the phase between the exciting sub pulses.

Keywords: tailor-shaped laser pulses, ionization process, superfluid helium droplets, wave packet interference

Introduction

During recent years spectroscopic studies of doped superfluid helium droplets have been an ever expanding field. Their unique properties make these cold droplets an ideal tool for e.g. studies on superfluid properties in finite systems, high resolution molecular spectroscopy, weakly bound complex formation, and recently even regarding the dynamics of the doped molecular

*Corresponding author

Email address: lindin@physik.fu-berlin.de (Albrecht Lindinger)

[1]École polytechnique, Route de Saclay, 91128 Palaiseau, France

[2]Institut für angewandte Physik, Universität Bern, Sidlerstrasse 5 CH-3012 Bern, Switzerland

[3]Institut für Ionenphysik und Angewandte Physik, Universität Innsbruck, Innsbruck, Austria

constituents. A number of research groups contributed to the field and the progress is reported in overview articles [1, 2].

Helium droplets can be regarded as a unique matrix since they enable free rotation of the embedded molecules, they only marginally influence the molecular properties, and they provide efficient cooling of the internal degrees of freedom. From the spectroscopy of the embedded molecules, information can be gained about the molecular structure or the interaction with the surrounding helium matrix, and also about the properties of the superfluid matrix itself.

In spite of the large interest in this field, the potential of helium droplets for the synthesis of novel dopant complexes and the analysis of their unique dynamics upon ionization, excitation, and reaction has not been exhausted [3]. Particularly, the application of shaped laser pulses for coherent control of the molecular dynamics in helium droplets has not yet been conducted. Controlling the molecular dynamics with tailored laser fields [4, 6, 5, 7] will offer the unique possibility to investigate the induced processes in the superfluid finite environment.

Potassium dimers are well suited for the demonstration of coherent control and wavepacket interference on helium droplets since their photo-induced dynamics has been investigated by fs-spectroscopy in molecular beams [8, 9] and on helium droplets [10, 11]. It is known that they reside in bubble-like structures on the surface of the helium droplets [12, 13]. Potassium dimers preferentally form high-spin states on helium droplets but they also give rise to low-spin states which are expected to show characteristic wave packet dynamics after photo-excitation [11, 13, 14].

1. Experimental setup

The experimental equipment consists of three parts: a source of superfluid and supercold helium droplets used to pick up potassium atoms; a laser stage producing tailor-shaped pulses; and a detection zone. A schematic representation of these successive parts is given in Figure 1.

For the generation of helium droplets, we used ultrapure helium 6.0 which is cooled down in a gas cylinder before passing through the nozzle. The temperature and diameter of the nozzle, together with the pressure in the cylinder will determine the size of the droplets.

In our case, the nozzle is an orifice of 5 μm in a thin disk of platinum. The helium is prepared at 30 bar and the system is cooled down to 13.5 K

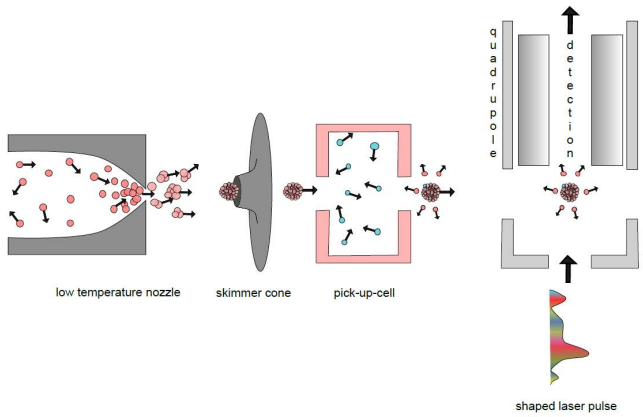

Figure 1: Schematic representation of the setup, including the helium droplet source, the pick-up cell and the detection unit.

by a closed-cycle helium cryostat, CTI-Cryogenics model 8300. A Lakeshore 331 temperature controller and a silicon diode glued to the cylinder ensure thermal stabilization by heating the system if necessary.

Those parameters allow for the generation of droplets of $\sim 10^4$ atoms ($\sim 10^2$Åin diameter). After the nozzle, droplets are formed by gas expansion, and their temperature drops quickly to 0.37 K [1]. The vacuum pump is efficient enough to ensure a high vacuum of $10^{-4} - 10^{-5}$ mbar in the source chamber, which corresponds to a mean free path of 1-10 m. A skimmer provides directional selectivity.

After the skimmer, the helium droplet jet enters the pick-up chamber and picks up the species by passing through holes in the oven where the potassium is heated. The temperature of the oven is set in order to adjust the potassium pressure and thus to optimize the probability for a droplet to pick up two potassium atoms. Finally the droplets reach the detection chamber.

The laser pulses are prepared in an adjacent room. We use a Ti:Sa Mira - Coherent laser generating pulses with an energy of 10 nJ, a repetition rate of 76 MHz, and a central wavelength tunable in the near-IR. The Mira is pumped by a Nd:VYO_4 continuous Verdi - Coherent laser at 532 nm.

The pulses are shaped by a commercial spatial light modulator (SLM-640, Cambridge Research & Instrumentation) with two liquid crystal arrays having 640 pixels of 100 μm each, in a $4f$-setup, consisting of two diffraction

gratings of 1200 lines/mm and two cylindrical lenses of 250 mm focal length.

The pulse shaping enables us to generate single pulses, with or without chirp, as well as multiple pulses, with tunable delay and phase difference between them [15]. We can also optimize the shape of the pulse; to this purpose, a genetic algorithm and alternatively the pulse optimization method PRISM [16] were implemented.

The detection chamber has windows on the sides, by which the laser enters the chamber and crosses the helium beam right below the detection device. The quadrupolar mass analyzer (BALZERS QMA 400) detects the ions created by the action of the laser pulses on the potassium dimers.

2. Results

Since we can produce tailor-made pulses or sequences of pulses, we can do various experiments with our set-up. We present, at first, the chirp dependence of the mass detection, and then pump-probe experiments.

2.1. Chirp dependence of cluster ionization

The following measurements are made with laser pulses at 805 nm center wavelength with and without linear chirp, having a FWMH of approximately 50 fs for the transform-limited pulse. We adjusted the pressure in the pick-up cell in order to maximize the number of droplets carrying a potassium dimer. The amount of differently sized potassium clusters is lower but non-zero, so that we can also study the behavior of monomers and trimers.

Figure 2 presents the chirp-dependence of the ion yield as a function of the chirp parameter $b_2 = \mathrm{d}^2\psi(\omega)/\mathrm{d}\omega^2|_{\omega_0}$ of the spectral phase. The dispersion accumulated by the laser beam on its optical path to the interaction zone has been compensated, so that the zero of the chirp axis corresponds to a non-chirped pulse. It can be clearly seen that the linear chirp has a different influence on the ionization of monomers, dimers and trimers. We notice the following characteristic features:

– Around zero chirp, we observe a dip in the dimer signal curve. This is probably due to the fact that the peak intensity of the pulse near its tranform-limited conditions (i. e. without chirp) is higher and causes fragmentation of the dimers mainly in the ionic state, since at this high peak intensity further excitation will occur in the ionic state which leads to subsequent fragmentation of the molecular ion [17]. The feasibility

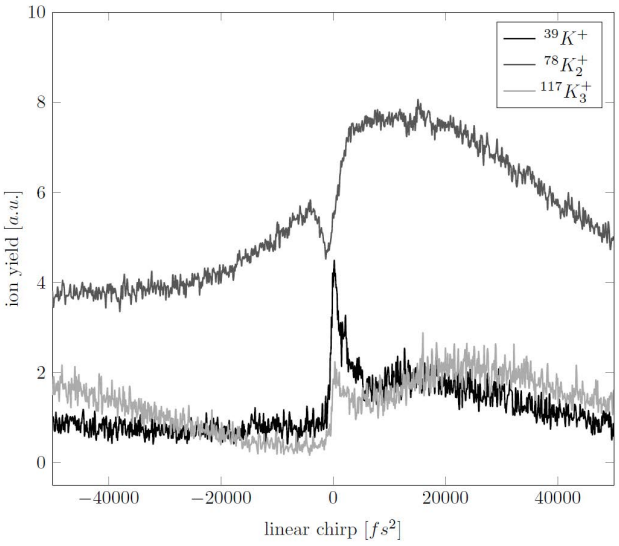

Figure 2: Chirp dependence: ion yields for the potassium monomer (black), dimer (dark gray) and trimer (light gray) are depicted depending on the linear chirp of the laser pulse.

for reaching larger parts of the neutral excited potential energy curves by using longer pulses and hence achieving higher Franck-Condon factors may also be relevant [18]. It corresponds to a peak in the monomer signal, which has its maximum for the shortest pulses since a transform-limited pulse is expected to have the highest ion yield for multi-photon ionization of monomers.

– The positive chirp increases the dimer signal up to a maximum attained at 15 000 fs^2. This can be explained in the following way: a 50 fs pulse with an additional 15 000 fs^2 chirp has its duration multiplied by a factor of about 6. The pulse will be as long as a half oscillation period on the $A^1\Sigma_u^+$ state, allowing the wave packet to reach the outer turning point (see Figure 3 (I)). Apparently, a positive chirp with the initial low frequencies, preparing low vibrational states in the first excited state, and higher frequencies for the second excitation step is more efficient than vice versa. This can mainly be attributed to the more favorable Franck-Condon factors in the temporal evolution of the ionization process for positive chirp [18]. Particularly, a vibrational state distribution shift may be relevant in our chip dependent results, similar as described in [19]. This could shift the vibrational distribution to lower values for

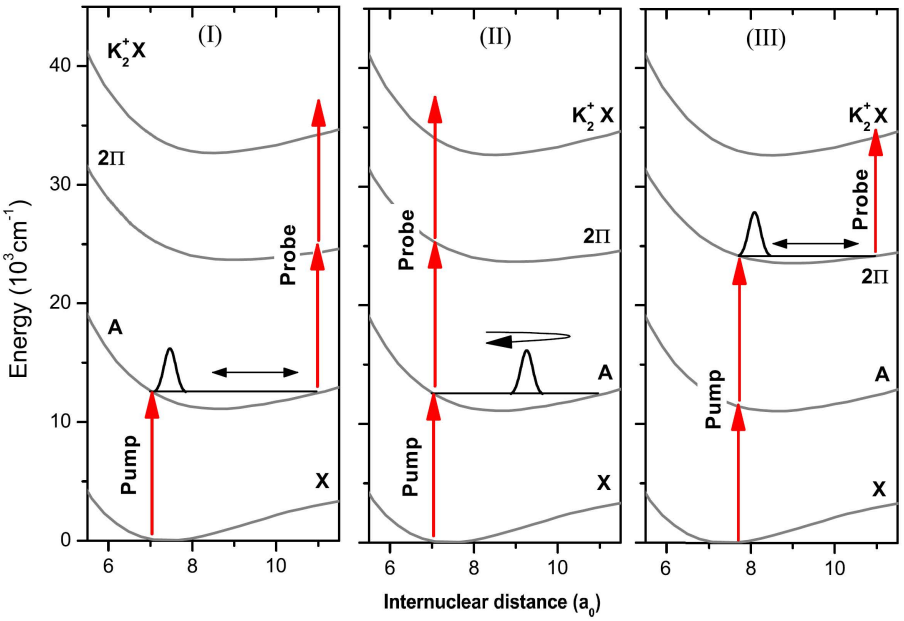

Figure 3: Possible pathways for ionization of K_2. Image adapted from [11].

positive chirps which leads to stronger bound alkali dimers and hence increased dimer ion signal.

– For a chirp between 0 and +5000 fs^2, we notice a broad dip of the trimer signal (and a concomitant increase of monomer signal), corresponding to trimer fragmentation [20]. Contrary to the ionization of dimers proceeding via bound neutral excited states, unbound neutral excited states are reached for trimers which leads to fragmentation at these chirp conditions.

Therefore, the chirp depencence of the ionization dynamics of potassium monomers, dimers, and trimers is comprehensible by reason of the given explanations based on the involved potential curves.

2.2. Pump-probe experiments

The pump-probe experiments consist of exciting the dimer, initially in a known state, with a pump pulse, and after a delay, putting it in a measurable state with a probe pulse. The production of the two delayed sub pulses is

made by spectral means with the shaper. This is more precise than a delay line but does not allow for very long delays.

The initial state of the potassium dimers embedded in helium droplets is the lowest vibrational state in the $X^1\Sigma_g^+$ ground state of K_2, while the detectable state is the $X^2\Sigma_g^+$ ground state of K_2^+. Between these two, various pathways exist, which can be evaluated with the help of the Franck-Condon principle. Depending on the wavelength, one or various of them will be present. The excitation can take place from or via singlet or triplet states. We do not have indications for a contribution from triplet states but we cannot exclude this. The main oscillations are attributed to the singlet $A^1\Sigma_u^+$ and $2^1\Pi_g$ states, also according to former work [11]. Further oscillations, e.g. in the $b^3\Pi$ state or the singlet ground state may occur but remain insignificant and cannot be assigned from our experimental data. Examples of pathways via potential energy curves from [21] are shown in Figure 3, adapted from the work of Stienkemeier *et al.* [2]:

- Pathway (I) is the excitation by the pump to the first excited level, followed by an oscillation of the wave packet in the $A^1\Sigma_u^+$ state. This oscillation has a frequency of 65 cm^{-1} (period 0.51 ps). It is followed by a two-photon step transition via the resonant state 2Π. This scheme applies from $\lambda = 850$ nm to 810 nm, where the Franck-Condon window between the $A^1\Sigma_u^+$ and $2^1\Pi_g$ states switch from the outer turning point to the inner turning point [11].

- Pathway (II) is quite similar to the pathway (I), but the two-photon ionization takes place at the inner turning point because of a shift of the Franck-Condon window. The oscillation has the same frequency as in (I). This scheme is active for wavelengths around 780 nm.

- Pathway (III) begins by the absorption of two photons of the pump pulse, followed by an ionization with one photon of the probe pulse. An oscillation takes place in the 2Π state, with 45 cm^{-1} frequency (period 0.74 ps)[11]. This scheme occurs for $\lambda \sim$ 780–800 nm

- Other pathways exist, as for instance an excitation of the wave packet in the ground state X at frequency 92 cm^{-1} (period 0.36 ps) [11] followed by a three-photon ionization (active at higher laser intensity, for λ between 780 and 820 nm).

Those pathways can simultaneously be present and the resulting dynamics can be analyzed by means of pump-probe experiments. Our pump-probe scans provide a higher temporal resolution than in former work [11] which particularly enables to reveal the dynamics close to zero delay. The pump-probe measurements are read in the following way. For $t > 0$, the first pulse comes at $-t/2$ and the second pulse comes at $t/2$.

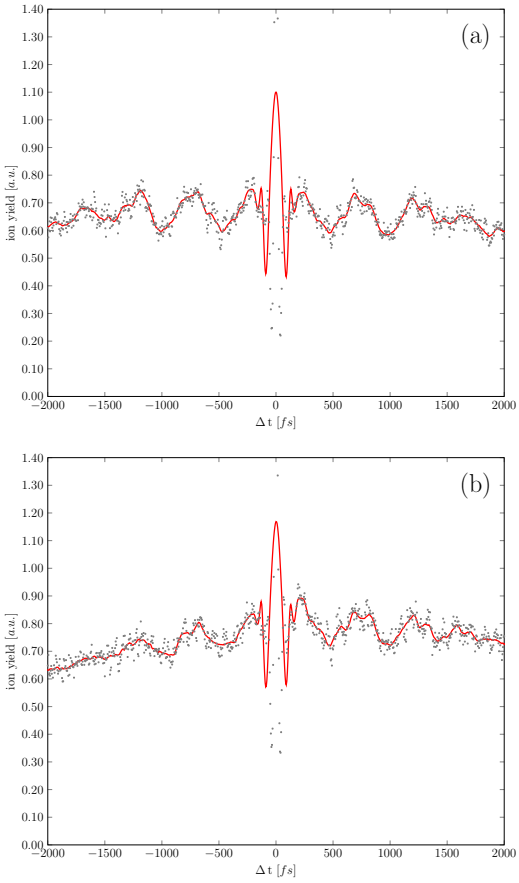

Figure 4: Pump-probe scans of the ionization of potassium dimers on helium droplets. The $^{78}K_2^+$ signal is recorded and the center wavelength amounts to 827 nm. The solid line shows a fifth order spline fit with 50 points averaging. (a) Pump and probe pulses have the same intensity. (b) Pump and probe pulses have an intensity ratio of four. It can be observed that in this case positive delays induce oscillations with larger amplitudes than negative delays.

2.2.1. Intensity difference

A way to enhance or inhibit paths is to modulate the respective amplitudes of pump and probe. Two-photon ionization, even in this resonant configuration, is favored when the intensity is high. So, a stronger pump followed by a weaker probe is expected to enhance the path (III), whereas a weaker pump and a stronger probe would boost path (I) and (II).

The graph in Figure 4(a) is measured by using identical pump and probe pulses, whereas in the Figure 4(b), we show the measurement made with a pump-probe intensity ratio of 4. Thereto, the intensity of one sub pulse is reduced accordingly by amplitude modulation. We tuned the central wavelength of the laser to 827 nm, where the scheme (I) is dominant, and used a pulse length of ~ 50 fs FWHM, as can be seen on the peak at $t = 0$ fs, being the cross-correlation of the two pulses.

The curve in Figure 4(a) is symmetric with respect to zero delay, because for negative delays pump and probe exchange their role, given that they have same intensity and phase. We observe signal oscillations with an oscillation period of 500 fs. The first maximum is at a pulse delay of the half oscillation period at 250 fs which clearly indicates ionization on pathway (I).

In Figure 4(b), we observe that the symmetry is broken. A positive delay induces oscillations with larger amplitudes than a negative delay. This can be explained with the most efficient sequence for the active path (I) involving a weak pulse for the 1-photon step $X \rightarrow A$ followed by a strong pulse for the 2-photons step $A \rightarrow \Pi \rightarrow$ ion. Hence, the different power dependence of the first and second excitation step is responsible for the asymmetry. It should be mentioned that other processes like ionization from each pulse alone are responsible for the constant background. The weak dependence on the changed relative intensities is somehow surprising. It may be explained by partial saturation of the excitation transitions (e.g. almost total saturation of the first and partial saturation of the second excitation step, leading to a weak dependence on the power mainly of the second excitation step.).

2.2.2. Phase shift

We perform pump-probe scans of potassium dimer ion signals by changing the phase difference between the two sub pulses from zero to π. Using a pulse shaper for pulse generation enables to precisely tune the phase difference between the sub pulses. For these measurements, the central laser wavelength was set to 790 nm, where paths (II) and (III) are expected to be active. Ground state oscillations induced by resonant impulsive stimulated Raman

scattering are minor due to the low pulse energies of the laser oscillator. Therefore they are not regarded but in principle they should be present. In Figure 5(a) we show a pump-probe scan, with pump and probe being identical and a phase shift of zero, whereas in Figure 5(b), we introduce a phase shift of π between pump and probe, the intensities being equal. The sub pulse durations were 50 fs in both cases.

We observe oscillations in the potassium dimer ion signal. Figure 5(a) exhibits a rich non-regular oscillation pattern, which makes us predict that apparently several differing oscillation periods are involved. A significantly modified ion signal with a single oscillation of T $\approx$ 800 fs was observed in Figure 5(b) by only varying the phase difference.

This observation, attributed to a notably changed ionization process, can be explained with the following proposed scenario. For the zero phase difference the wave packet oscillation in the first excited $A^1\Sigma_u^+$ state and pathway (III) are believed to be present simultaneously. The initial excitation to the $A^1\Sigma_u^+$ state is at the inner turning point and the further excitation and ionization occurs close to the inner turning point but shifted to larger internuclear distance [9]. The wave packets interfere thereby constructively due to the zero phase difference since the molecular wave packet inherits the phase of the pulse which produced it.

In contrary to that, for the phase difference of π one gets destructive interference in the first excited state since the first molecular wave packet destructively interferes with the wave packet induced by the second sub pulse, which results in a decreased signal. More precisely, the involved wave functions add constructively or destructively depending on the phase difference, according to the fundamental work of Scherer *et al.* [22]. Hence, one ionization path is clearly removed in the case of the π phase shift. Yet, the ionization path via the second excited $2^1\Pi_g$ state is still utilized in this case (as well as for zero phase difference since the oscillation in the $2^1\Pi_g$ state is obtained in both cases). This longer oscillation period is consistent with an oscillation in the $2^1\Pi_g$ state and it is as well obtained as a peak in both Fourier transformed signals at about 45 cm^{-1} (see Figure 6). Therefore, a phase shift between different sub pulses results in a remarkably different ionization process via different excited states.

It is interesting to note that in the π-shifted case, the zero delay in the pump-probe scan corresponds to a minimum for the 800 fs oscillation and the first maximum is present at about half the oscillation period. Thus, the initial excitation occurs at the inner turning point and the further excitation

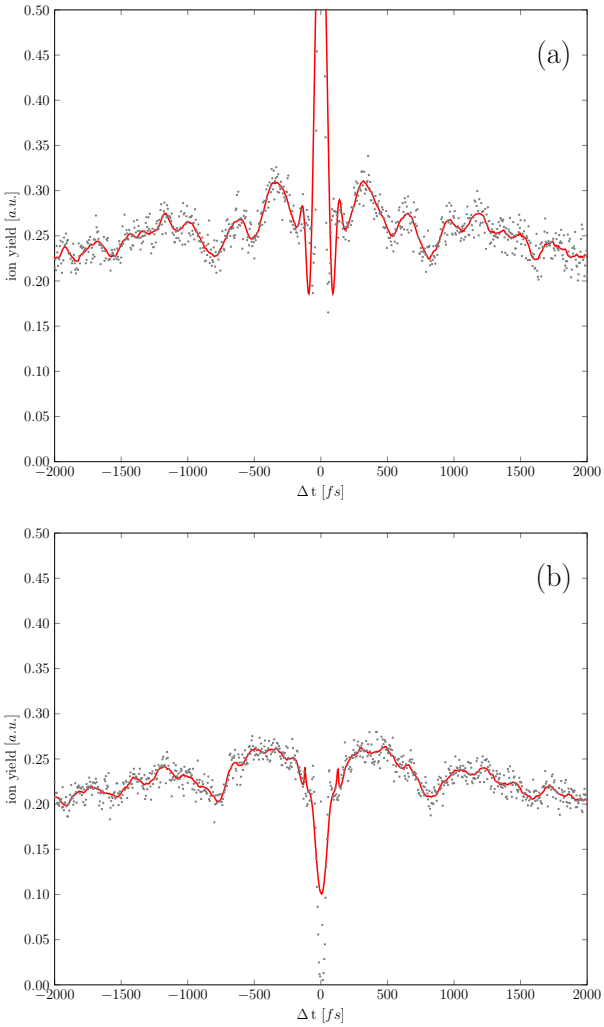

Figure 5: Pump-probe scans of the ionization of potassium dimers on helium droplets. The $^{78}K_2^+$ signal is recorded, the center wavelength amounts to 790 nm. The solid line shows a fifth order spline fit with 50 points averaging. (a) The phase difference between the two sub pulses is zero. (b) The phase difference between the two pulses amounts to π. A significant change is observed by only altering the phase difference which can be attributed to a remarkably differing wave packet dynamics.

and ionization at the outer turning point. This proves that the wave packet has to perform a half cycle in the 2Π state to reach the most favorable zone for ionization, the outer turning point, thereby confirming the (III) scheme.

The fast signal modulation for the zero phase shift can be explained by

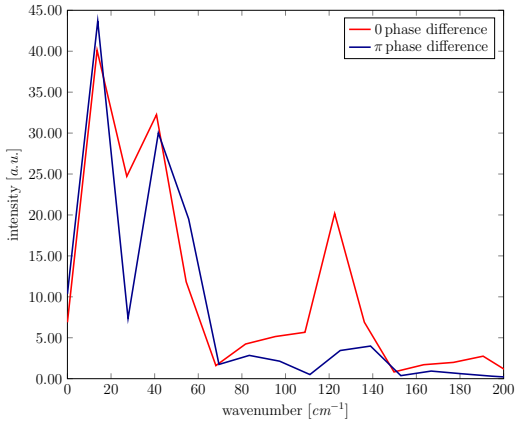

Figure 6: Fourier transforms of the pump-probe scans of the ionization of potassium dimers on helium droplets. The peak at about 125 cm^{-1} is missing in the case of the π phase difference.

further excitation from the $A^1\Sigma_u^+$ state at larger internuclear distances than the inner turning point. This results in passing the Franck-Condon window twice during one oscillation period, similar as explained by Nicole *et al.* [9]. This fast modulation can be observed in the Fourier transform of the pump-probe scans (see Figure 6) at about 125 cm^{-1}. This peak in the Fourier spectrum is clearly removed by shifting the phase difference to π. From these experimental observations it is apparent that the wave packets destructively interfere, although the first and second molecular wave packet are not exactly at the same internuclear distance. Yet, due to these findings they are believed to be already close enough for substantial destructive interference. At the examined short time delays the dimers are still attached to the droplet surface (see [14]), and hence we demonstrated that the coherence is maintained for coherent control despite the damping by the helium matrix.

3. Conclusions

In this article, coherent control for molecules embedded on helium droplets was demonstrated. We observed different pump-probe signatures depending on the intensity ratio of the sub pulses which provided insight into the ionization process. Particularly, it was proven that it is possible to perform a selection between ionization paths for potassium dimers on superfluid helium droplets by using shaped laser pulses. We interpreted this feature as

follows: the pathway via the $A^1\Sigma_u^+$ state is involved when pump and probe have the same phase since the wave packets interfere thereby constructively, but is annihilated when there is a π shift introduced between both pulses which generates opposite wave packets and hence destructive interference. We provided an explanation based on the work of Scherer *et al.* [22] assuming that the wave packet inherits the phase of the pulse which produced it. For the zero phase shift, the dynamics has two main frequency components due to the two pathways, whereas for the π phase shift, only the frequency corresponding to the pathway (III) drives the dynamics.

This experiment can be regarded as a demonstration of wave function interference control proposed by Shapiro *et al.* [23] and in particular of phase-locked pump-probe performed by Scherer *et al.* [22], but specifically for molecules on helium droplets and with a drastic change of the excitation path. This proves that the coherence is sustained for molecules on helium surfaces and can be considered as a step towards deeper insight into molecular coherent control on helium droplets.

Acknowledgments

We thank Professor L. Wöste for his support and advice. DFG and FWF are acknowledged for financial support (D-A-CH project number I 978).

[1] J. P. Toennies and A. F. Vilesov, Angew. Chem. Int. Ed. **43**, 2622 (2004).

[2] F. Stienkemeier and K. K. Lehmann, J. Phys. B: At. Mol. Opt. Phys. **39**, R127 (2006).

[3] C. Giese, T. Mullins, B. Grüner, M. Weidemüller, F. Stienkemeier, and M. Mudrich, J. Chem. Phys. **137**, 244307 (2012).

[4] P. Brumer and M. Shapiro, Rep. Prog. Phys. **66**, 859 (2003).

[5] T. Brixner and G. Gerber, ChemPhysChem **4**, 418 (2003).

[6] A. Assion, T. Baumert, M. Bergt, T. Brixner, B. Kiefer, V. Seyfried, M. Strehle, G. Gerber, Science **282**, 919 (1998).

[7] A. Lindinger, C. Lupulescu, M. Plewicki, F. Vetter, S. M. Weber, A. Merli, and L. Wöste, Phys. Rev. Lett. **93**, 033001 (2004).

[8] S. Rutz, R. de Vivie-Riedle, and E. Schreiber, Phys. Rev. A **54**, 306 (1996).

[9] C. Nicole, M. A. Bouchene, C. Meier, S. Magnier, E. Schreiber, and B. Girard, J. Chem. Phys. **111**, 7857 (1999).

[10] J. H. Reho, J. P Higgins, and K. K. Lehmann, Faraday Discuss. **118**, 33 (2001).

[11] P. Claas, G. Droppelmann, C. P. Schulz, M. Mudrich, and F. Stienkemeier, J. Phys. B: At. Mol. Opt. Phys. **39**, S1151 (2006).

[12] L. An der Lan, P. Bartl, C. Leidlmair, H. Schbel, S. Denifl, T. D. Mrk, A. M. Ellis, and P. Scheier, Phys. Rev. B **85**, 115414 (2012).

[13] J. Higgins, C. Callegari, J. Reho, F. Stienkemeier, W. E. Ernst, M. Gutowski, and G. Scoles, J. Phys. Chem. **102**, 4952 (1998).

[14] M. Schlesinger, M. Mudrich, F. Stienkemeier, and W. T. Strunz, Chem. Phys. Lett. **490**, 245 (2010).

[15] S. M. Weber, A. Lindinger, F. Vetter, M. Plewicki, A. Merli, and L. Wöste, Eur. Phys. J. D **33**, 39 (2005).

[16] T. Wu, J. Tang, B. Hajj, and M. Cui, Opt. Express **19**, 12961 (2011).

[17] A. Lindinger, A. Merli, M. Plewicki, F. Vetter, S. M. Weber, and L. Wöste, Chem. Phys. Lett. **413**, 315 (2005).

[18] A. Bartelt, A. Lindinger, C. Lupulescu, V. Vajdaz, and L. Wöste, Phys. Chem. Chem. Phys. **5**, 3610 (2003).

[19] L. Levin, W. Skomorowski, L. Rybak, R. Kosloff, C. P. Koch, and Z. Amitay, Phys. Rev. Lett. **114**, 233003 (2015).

[20] S. Rutz, H. Ruppe, E. Schreiber, and L. Wöste, Zeitschrift für Physik D Atoms Molecules and Clusters **40**, 21 (1997).

[21] S. Magnier and Ph. Millie, Phys. Rev. A **54**, 204 (1996).

[22] N. F. Scherer, R. J. Carlson, A. Matron, M. Du, A. J. Ruggiero, V. Romero-Rochin, J. A. Cina, G. R. Fleming, and S. Q. Rice, J. Chem. Phys. **95**, 1487 (1991).

[23] C. K. Chan, P. Brumer, and M. Shapiro, *J.Chem. Phys.* **94**, 2688 (1991).